tvst
Retina

A Simple and Rapid Method for Simultaneous Isolation of Mouse Retina and RPE Wholemounts

Jialiang Yang[1,*], Haiping Wu[1,*], Qi Li[1,*], Jiaxin Guo[1], Jialin Yao[1,2], Shengliu Pan[3,4], Xiawei Wu[1], Haotian Huang[1], Runfang Chen[1], Junnian Chen[1], Yubin Wang[1], Yue Peng[1,5], Fuhua Wu[1], and Jing Hu[1,5]

[1] Sichuan Provincial Key Laboratory for Human Disease Gene Study, Department of Laboratory Medicines, Sichuan Provincial People's Hospital, University of Electronic Science and Technology of China, Chengdu, China
[2] Department of Clinical Pharmacology, College of Pharmacy, Dalian Medical University, Dalian, China
[3] Center for Natural Products Research, Chengdu Institute of Biology, Chinese Academy of Sciences, Tianfu New District, Chengdu, China
[4] The University of Chinese Academy of Sciences, Huairou District, Beijing, China
[5] School of Medicine, University of Electronic Science and Technology of China, Chengdu, China

Correspondence: Jing Hu, The Sichuan Provincial Key Laboratory for Human Disease Gene Study, Sichuan Provincial People's Hospital, University of Electronic Science and Technology of China, 32 The First Ring Rd. West 2, Chengdu, Sichuan 610072, China. e-mail: jinghu_somed@uestc.edu.cn
Fuhua Wu, The Sichuan Provincial Key Laboratory for Human Disease Gene Study, Sichuan Provincial People's Hospital, University of Electronic Science and Technology of China, 32 The First Ring Rd. West 2, Chengdu, Sichuan 610072, China. e-mail: wufuhua20160902@qq.com
Yue Peng, The Sichuan Provincial Key Laboratory for Human Disease Gene Study, Sichuan Provincial People's Hospital, University of Electronic Science and Technology of China, 32 The First Ring Rd. West 2, Chengdu, Sichuan 610072, China. e-mail: ruipeng1215@163.com

Received: December 31, 2024
Accepted: March 28, 2025
Published: May 12, 2025

Keywords: retina; retinal pigment epithelium (RPE); wholemounts; isolation; ophthalmic disease

Purpose: Retina and retinal pigment epithelium (RPE) wholemounts are important models for studying the pathophysiology of retinal-related ophthalmic diseases, such as age-related macular degeneration and diabetic retinopathy. Currently, there is no method available for simultaneously obtaining retina and RPE wholemounts. The aim of this study is to develop a simple, rapid, and effective technique for the simultaneous isolation of mouse retina and RPE wholemounts.

Methods: We developed a novel, streamlined procedure for the efficient isolation of intact retina and RPE wholemounts from mouse eyes. The method involves minimal dissection and uses basic laboratory equipment, allowing the entire process to be completed in approximately 2 to 5 minutes per sample. The study also explores the impact of different fixation times on the structural integrity and quality of both retina and RPE wholemounts (3 hours in 4% paraformaldehyde [PFA], 30 minutes $< 1 \times$ phosphate-buffered saline [PBS] $<$ 3 hours).

Results: The new method consistently yields high-quality, intact retina and RPE wholemounts, with excellent structural integrity suitable for downstream imaging and molecular analyses. The technique significantly reduces preparation time. Optimal fixation conditions were identified, with 3 hours of fixation in 4% PFA and PBS incubation times between 30 minutes and 3 hours yielding the best results. The approach showed higher tissue integrity (80% vs. 45%) and improved staining quality of photoreceptor and ganglion cells. Additionally, the method is highly reproducible and effective for wholemount preparations from both young and older mice (6 and 12 months).

Conclusions: This study presents a significant advancement in the preparation of retina and RPE wholemounts. The simplicity, speed, and preservation of tissue integrity of the new method make it a valuable tool for ophthalmic disease research. Its potential applications include drug screening, gene therapy, and disease modeling, offering significant advantages in time efficiency, reproducibility, and the quality of morphological analysis.

Citation: Yang J, Wu H, Li Q, Guo J, Yao J, Pan S, Wu X, Huang H, Chen R, Chen J, Wang Y, Peng Y, Wu F, Hu J. A simple and rapid method for simultaneous isolation of mouse retina and RPE wholemounts. Transl Vis Sci Technol. 2025;14(5):14, https://doi.org/10.1167/tvst.14.5.14

Introduction

Ophthalmic diseases remain a leading cause of blindness globally, affecting millions of individuals.[1] The retina and retinal pigment epithelium (RPE) are key tissues involved in visual function and are central to the pathology of many ocular diseases.[1–4] The retina processes visual information by converting light into neural signals that are transmitted to the brain, whereas the RPE supports retinal function by maintaining photoreceptor health, absorbing scattered light, metabolizing waste, and participating in the visual cycle.[2,3] Recent studies have highlighted the critical role of retina-RPE interactions in the development and progression of diseases, such as age-related macular degeneration (AMD) and diabetic retinopathy.[4]

Retina wholemounts offer significant advantages over tissue sections, as they preserve the overall architecture of the retina, allowing researchers to observe structural and functional changes across different layers.[5,6] However, current techniques are inadequate for simultaneously isolating intact retina and RPE wholemounts, limiting our ability to study their interactions in disease models.[7]

This study aims to address this limitation by developing a rapid and straightforward method for simultaneously isolating retina and RPE wholemounts. Our technique reduces processing time, enhances tissue integrity, and is applicable in various research contexts, including disease modeling, drug screening, and gene therapy.[8]

Materials and Methods

The traditional method was performed as previously described.[5–8] Below is an introduction to the technique for the simultaneous isolation of mouse retina and RPE wholemounts.

The animal procedures were approved by the Institutional Animal Care and Use Committee (IACUC) of Sichuan Provincial People's Hospital and followed the guidelines of the Association for Research in Vision and Ophthalmology (ARVO) for the use of animals in research. C57BL/6J male mice (2, 6, and 12 months old) were used in this study. The overall procedure is illustrated in Figures 1 and 2. Details of the reagents and equipment used are provided in Tables 1, 2, and 3.

Healthy adult C57BL/6 J mice (8–16 weeks old, 20–30 g) were obtained from GemPharmatech LLC (Nanjing, China). The mice were confirmed to be in good health on the day of the experiment. Surgical instruments, including ophthalmic scissors, forceps, and eyeball tweezers, were sterilized. A 4% paraformaldehyde (PFA) fixative (Sigma-Aldrich, 158127) was prepared for tissue fixation. Mice were euthanized by intraperitoneal injection of ketamine (100 mg/kg) and xylazine (10 mg/kg) in a well-ventilated area, using gloves to ensure sterility and safety.[9]

After anesthetizing the mouse, they were placed in a supine position and securely held by hand. Using Vannas scissors (RWD, S11036-08), they were gently inserted along the fascia plane between the eyeball and the orbit, and gradually severed the fascia attachments around the eyeball, allowing the eyeball to gradually detach. Next, we slid the scissors to the posterior pole of the eyeball and severed the optic nerve fibers and posterior scleral fascia to completely extract the eyeball without the need for orbital dissection (see Fig. 1A). The excised eyeballs were immediately placed in pre-chilled 4% PFA fixative at 4°C to preserve cellular structures, with care taken to avoid over- or under-fixation (see Fig. 1B). After fixation, the eyeballs were gently rinsed with sterile phosphate-buffered saline (PBS; Gibco, 10010023).

On a sterile surface, a small hole was made at the corneoscleral junction using a 30 G needle (see Fig. 1D). The tips of the ophthalmic scissors were inserted through the hole, followed by the careful removal of the cornea and the gentle extraction of the lens with forceps (see Figs. 1C–F). The cornea- and lens-removed eyeball was placed under a dissecting microscope, and ophthalmic microsurgical scissors were used to divide the eyeball into four quadrants, cutting to approximately two-thirds depth toward the optic nerve head (see Figs. 1G–J). Consistency in

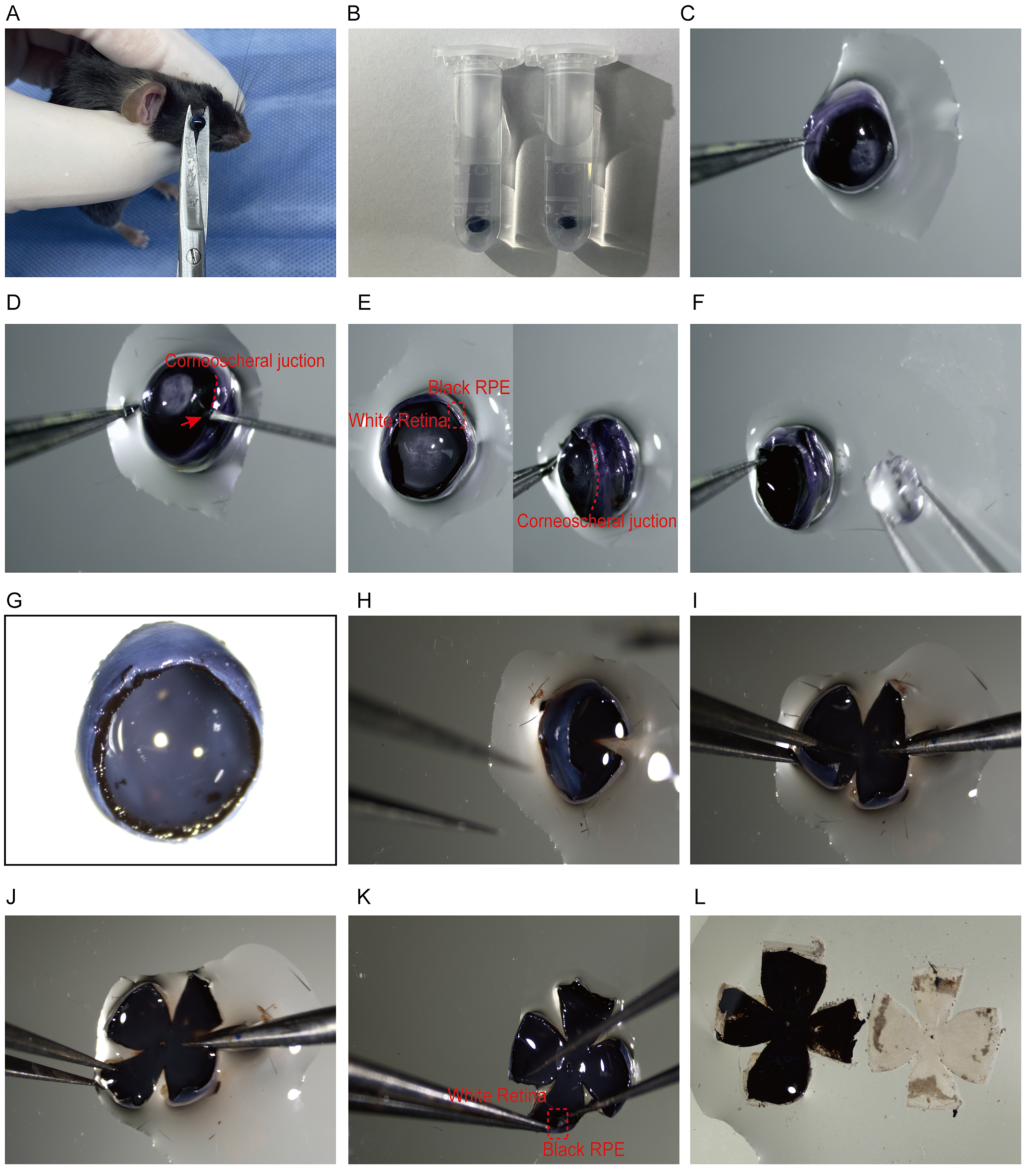

Figure 1. Flowchart for the preparation of retina and RPE wholemounts. (**A**) Following euthanasia, the mouse eyeball is carefully excised using ophthalmic scissors. (**B**) The eyeball is placed in 4% PFA fixative at 4°C for 20 to 30 minutes. (**C**) The eyeball is held in place by grasping its edge with ophthalmic forceps. (**D**) A small hole is made in the cornea using a 30 G needle. (**E**) The tips of the ophthalmic scissors are inserted through the hole, and the cornea is carefully removed. (**F**) The lens is gently extracted using hooked forceps. (**G**) The remaining eyeball is carefully placed under a dissecting microscope, with the eyecup facing upward. (**H–J**) The eyeball is evenly divided into four quadrants using ophthalmic scissors, ensuring that the cutting depth is approximately two-thirds from the edge toward the optic nerve head. (**K**) The retina and RPE layers are carefully separated along the margins using forceps or a brush. (**L**) The retina and RPE are gently flattened onto a glass slide, and excess tissue is carefully removed with a brush.

quadrant thickness facilitated the subsequent separation of the retina and RPE layers. The eyeball was positioned sclera-down under a microscope, and fine forceps were used to gently separate the retina from the RPE layer starting at the scleral margin, ensuring high-quality, intact wholemounts (see Fig. 1K). Throughout the procedure, the eyeball is kept moist with PBS but is not submerged. No supporting materials are required. The video demonstrates the entire process of the operation (Supplementary Video S1).

The separated retina and RPE wholemounts were gently placed on a glass slide using a fine brush. Subsequently, they were gently rinsed with PBS, and any residual tissue debris was carefully removed using the brush (see Fig. 1L). The wholemounts were then placed in 4% PFA fixative and stored at 4°C until further

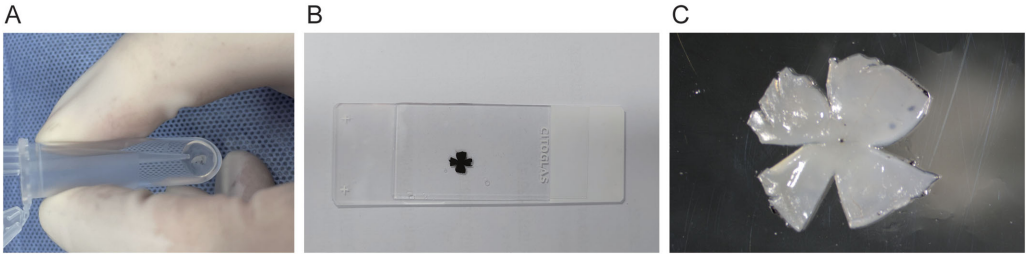

Figure 2. Flowchart for immunostaining retina and RPE wholemounts. (**A**) The immunostaining process is carried out in a 2 mL round-bottom EP tube, which serves as the staining container for all steps. (**B**) After staining, the RPE wholemount is carefully placed onto a glass slide, mounted with mounting medium, and observed under a microscope. (**C**) After staining, the retina wholemount is carefully placed onto a glass slide, mounted with mounting medium, and observed under a microscope.

Table 1. Reagents Used in the Experiment

Material Name	Brand/Supplier	Catalog Number
PFA	Sigma-Aldrich	158127
PBS	Gibco	10010023
NDS	Sigma-Aldrich	12352203

processing. If staining was not performed immediately, the specimens could be placed in ice-cold methanol and stored at –20°C. For immunofluorescence staining (see Fig. 2), samples were incubated with 5% donkey serum (NDS, Sigma-Aldrich, 12352203) for 30 minutes to 1 hour to block non-specific binding sites. Primary antibodies such as anti-S-opsin (Abcam, ab235274), Brn3a (Abcam, ab245230), and DAPI (Invitrogen, D21490) were incubated overnight at 4°C. After washing three times with PBS, fluorescent secondary antibodies (e.g. Alexa Fluor 488, Thermo Fisher, A-11008) were applied and incubated at room temperature for 1 to 2 hours. Samples were then washed again with PBS, and if nuclear staining was required, DAPI (Thermo Fisher, D 62248) was used. The retina or RPE was flattened on a slide under a dissecting microscope, a mounting medium was applied, and a coverslip was placed over the sample. Imaging was performed using a fluorescence or confocal microscope, with imaging settings optimized for each specific antibody used.

Table 3. Staining and Microscopic Observation Materials

Material Name	Brand/Supplier	Catalog Number
Anti-S-Opsin	Abcam	ab235274
Alexa Fluor 594	Thermo Fisher	A-11012
Alexa Fluor 488	Thermo Fisher	A-11008
DAPI	Thermo Fisher	62248
BRN3A	Abcam	ab245230
Anti-F-Actin	Invitrogen	MA1-80729
PNA	Invitrogen	L32459

Results

Effect of Fixation Time on Retinal Whole Mount Quality

In this study, we developed an efficient method for simultaneously obtaining wholemounts of mouse retina and RPE. In 82% of the experiments, we successfully isolated and fixed mouse retina and RPE wholemounts, which demonstrated good structural integrity, making them suitable for immunohistochemical staining and subsequent microscopic imaging.

To optimize the retinal fixation and processing steps, we explored the effect of different fixation times on

Table 2. Experimental Instruments and Consumables

Material Name	Brand/Supplier	Catalog Number
Sterile ophthalmic scissors	RWD (VANNAS/Spring Scissors/Straight/Fanned/Tapered, 8 cm)	S11036-08
Sterile tweezers	RWD (Fine Forceps /Straight, Tip 0.05 × 0.01 mm, 11 cm)	F11020-11
Centrifuge tubes	Thermo Fisher	90410
Microscope slides	CITOTEST	80302-0001

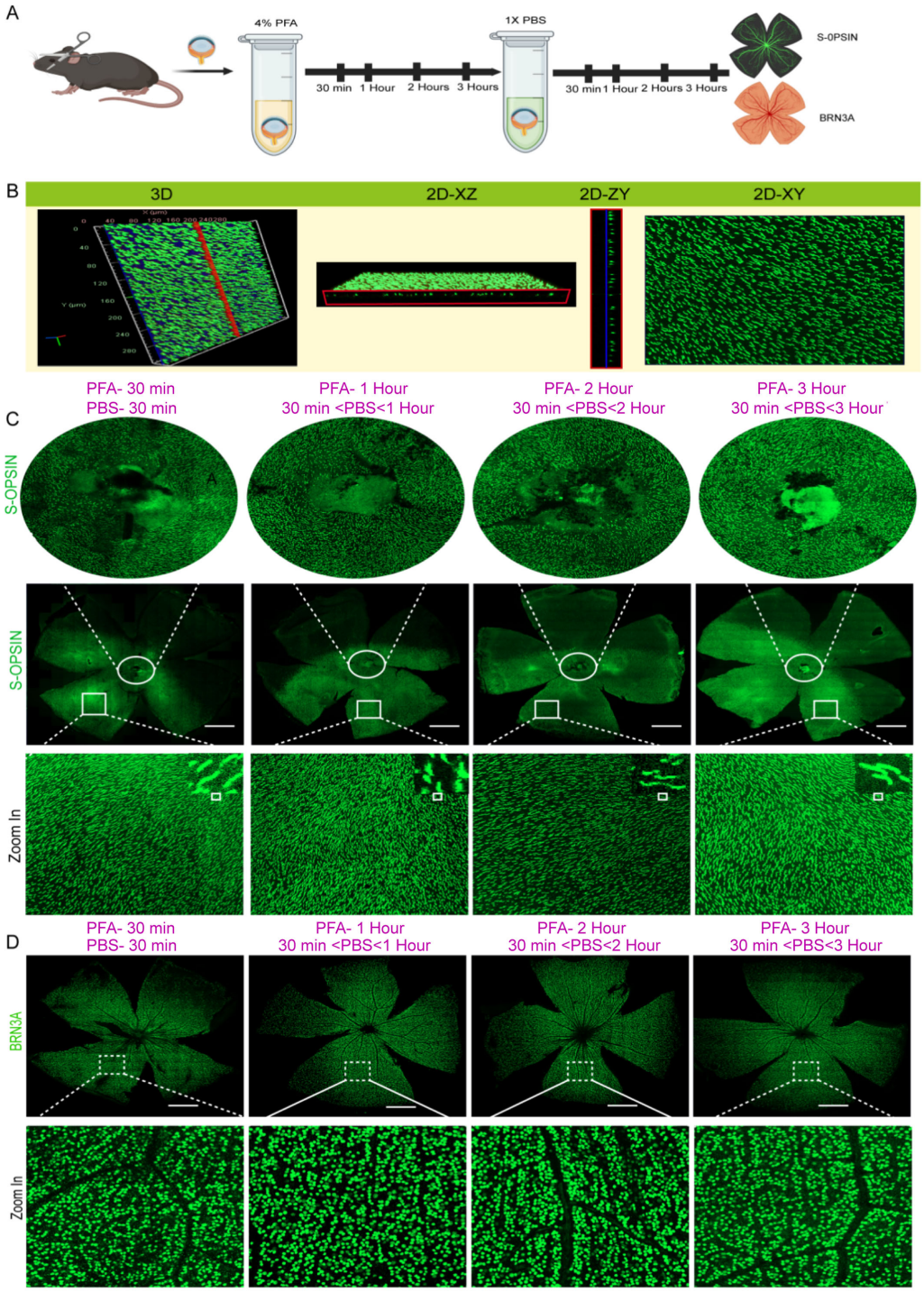

Figure 3. **Impact of fixation time on retina whole mount quality.** (**A**) Schematic representation of the effect of fixation time on retinal whole mount quality. (**B–D**) Retinal wholemounts labeled with S-opsin and Brn3a, showing the effects of different fixation times.

the quality of retinal wholemounts. Specifically, we compared fixation times in 4% PFA (30 minutes, 1 hour, 2 hours, and 3 hours) with different incubation times in 1× PBS (30 minutes, 1 hour, 2 hours, 3 hours, and 4 hours) to assess their impact on retinal integrity and morphology. Ten retinas were used for each group.

The results showed that both fixation time and PBS incubation time were critical for the quality of retinal wholemounts. When retinas were fixed in 4% PFA for 30 minutes, we designed PBS incubation times of 30 minutes and 1 hour. The results showed that when the PBS incubation time was within 30 minutes,

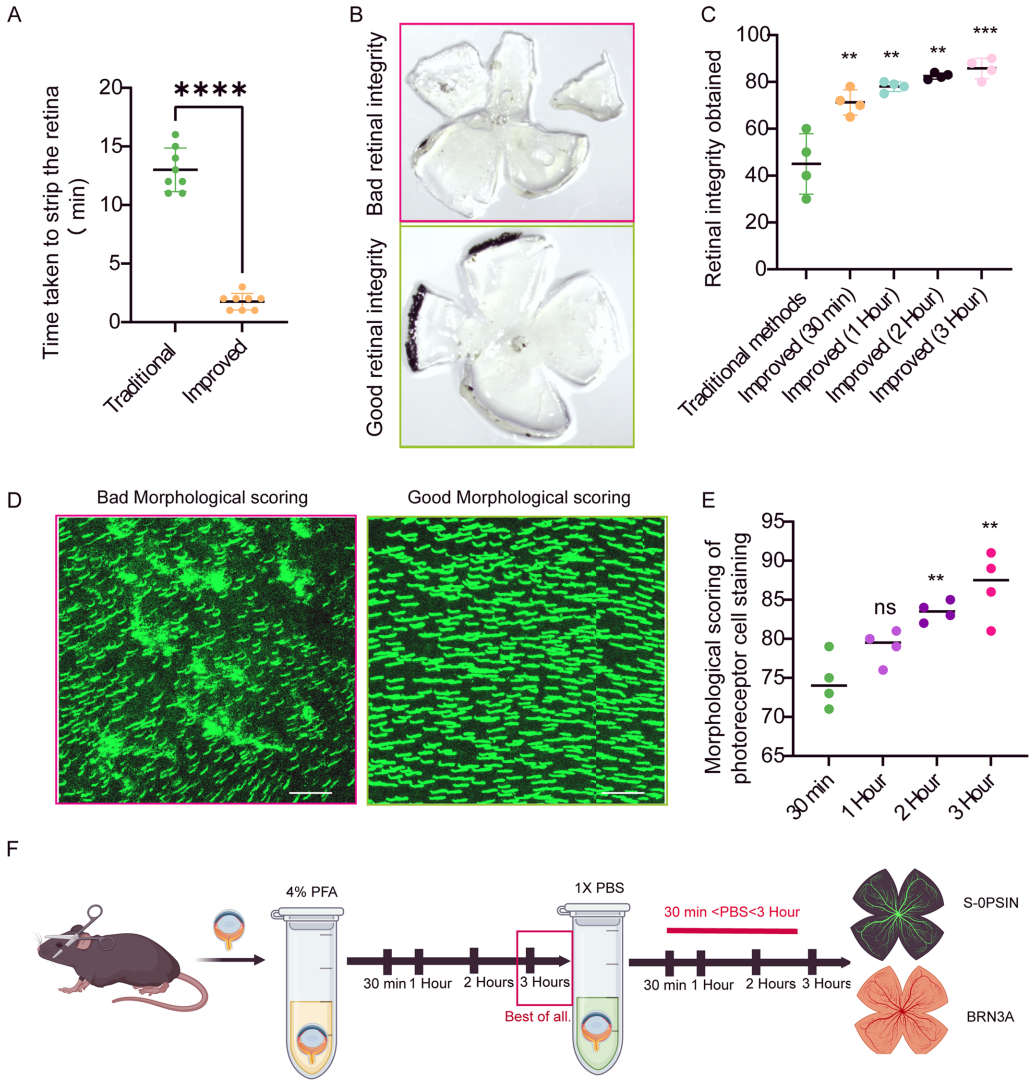

Figure 4. **Comparison between the new and traditional methods.** (**A**) Graph illustrating the time required to strip the retinas using both methods. (**B**) Representative images showing differences in retinal integrity (bad versus good). (**C**) Graph showing retinal integrity after processing with each method. (**D**) Representative images showing the morphological scoring differences of photoreceptor cell staining (bad versus good). (**E**) Graph depicting morphological scoring of photoreceptor cell staining for both methods. (**F**) Schematic representation of the optimal fixation time for achieving high-quality retinal whole mounts.

the retinal integrity was good; however, PBS incubation times longer than 30 minutes made the retina too soft, leading to breakage. When the fixation time was 1 hour, we designed PBS incubation times of 30 minutes, 1 hour, and 2 hours. The results showed that when PBS incubation times were between 30 and 60 minutes, retinal integrity was optimal; longer than 60 minutes caused the retina to become fragile. For fixation times of 2 hours, PBS incubation times of 30 minutes, 1 hour, 2 hours, and 3 hours were tested. The results showed that PBS incubation times within the range of 30 minutes to 2 hours preserved retinal integrity, whereas PBS incubation times longer than 2 hours resulted in breakage. For a fixation time of 3 hours, we tested PBS incubation times of 30 minutes, 1 hour, 2 hours, 3 hours, and 4 hours. The results showed that PBS incubation times within the range of 30 minutes to 3 hours maintained retinal integrity, whereas times longer than 3 hours caused the retina to break apart (Fig. 3A).

We used S-OPSIN antibody to label cone photoreceptors[10] and BRN3A antibody to label retinal ganglion cells for immunohistochemical staining.[8] The effect of different fixation and PBS incubation times on the staining results was observed. For the retinas of adult mice, the distribution of cone photoreceptors was highly uneven, with about one-third of the retina almost devoid of cone photoreceptors (Figs. 3B, 3C).

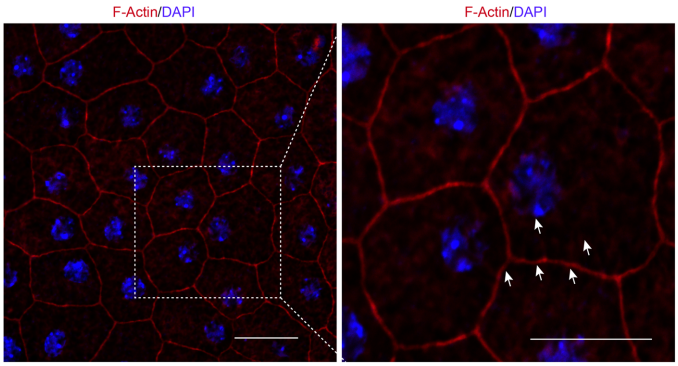

Figure 5. RPE wholemount labeled with F-Actin. *Left*: F-Actin (*red*) and DAPI (*blue*) labeling of the RPE. *Arrows* indicate areas of strong F-Actin signal. *Scale bar* = 10 µm. *Right*: Enlarged image of the corresponding area, showing detailed F-Actin (*red*) and DAPI (*blue*) labeling, with focus on actin filaments. *Scale bar* = 10 µm. *Arrowhead* annotation features are associated with increased scores.

Based on this, it is challenging to fully assess the pathophysiological state of the retina using sectioning methods, which may even lead to erroneous conclusions.

Through S-OPSIN antibody labeling, the results indicated that fixation for 3 hours with PBS incubation times greater than 30 minutes but less than 3 hours provided the best staining of cone photoreceptors. The cell morphology was more complete, and the peripheral morphology was smoother (see Figs. 3B, 3C). Similarly, retinal ganglion cell staining results showed that fixation for 3 hours with PBS incubation times greater than 30 minutes but less than 3 hours resulted in stronger staining intensity, lower background staining, and smoother nuclear morphology (Fig. 3D). At the same time, the fixation time may need to be appropriately adjusted based on different genetic backgrounds and/or experimental methods, in order to ensure the reliability and consistency of the experimental results.

Comparison of New Method With Traditional Method

We further compared the application of the new method with the traditional method in retinal wholemount preparations. First, the time spent by the three operators using the standard method showed no statistical differences, indicating consistency in their operational skills when using the standard method. Similarly, the time spent using the new method also showed no statistical differences, further indicating consistency among the operators within each method. Subsequently, each operator performed the experiment using both the standard and new methods, and the results of the two methods were compared and analyzed. The timing was carried out by an independent third-party person to ensure fairness and accuracy in the timing. Throughout the entire experiment, all procedures were performed blindly to ensure the objectivity and accuracy of the data. The traditional method takes approximately 12 minutes to complete the process from fixed eyeball to unstained retinal wholemounts,[6,11–13] whereas the new method only takes 2 minutes (Fig. 4A). Assessment of wholemount integrity showed that the new method (80%) was significantly superior to the traditional method (45%). Particularly, when the retina was fixed in 4% PFA for 3 hours and incubated in PBS for more than 30 minutes but less than 3 hours, the integrity of the resulting retina was the highest, averaging 82% (Figs. 4B, 4C).

Additionally, we compared the integrity of photoreceptor cell morphology based on different fixation times. The results showed that for a fixation time of 3 hours, when the PBS incubation time was greater than 30 minutes but less than 3 hours, the morphology of photoreceptor cell staining was improved, with smoother peripheral morphology (Figs. 4D–F).

These results indicate that the new method significantly reduces the processing time and improves both the retinal wholemount integrity and the quality of subsequent staining.

Evaluation of RPE Whole Mount Quality

For the simultaneously obtained RPE wholemounts, we used F-actin to label the cell membranes and DAPI to stain the nuclei. The results showed that F-actin labeling provided clear and intact RPE cell membrane morphology, allowing accurate differentiation of RPE cell shape, size, and structural integrity. This labeling is useful for evaluating the structure and function of the RPE. DAPI staining also demonstrated a good signal-to-noise ratio, enabling precise quantification of DAPI-positive cells in each RPE cell, which facilitates the assessment of RPE results and functionality (Fig. 5).

Application of Retinal Whole Mounts in Mice of Different Ages

We also conducted experiments on older mice (6 months and 12 months). Because photoreceptor cells are more difficult to stain and obtain complete morphological images compared with retinal ganglion cells, we selected the more challenging photoreceptor cells and used the new method to label photoreceptors in the retina. The retinal wholemount results

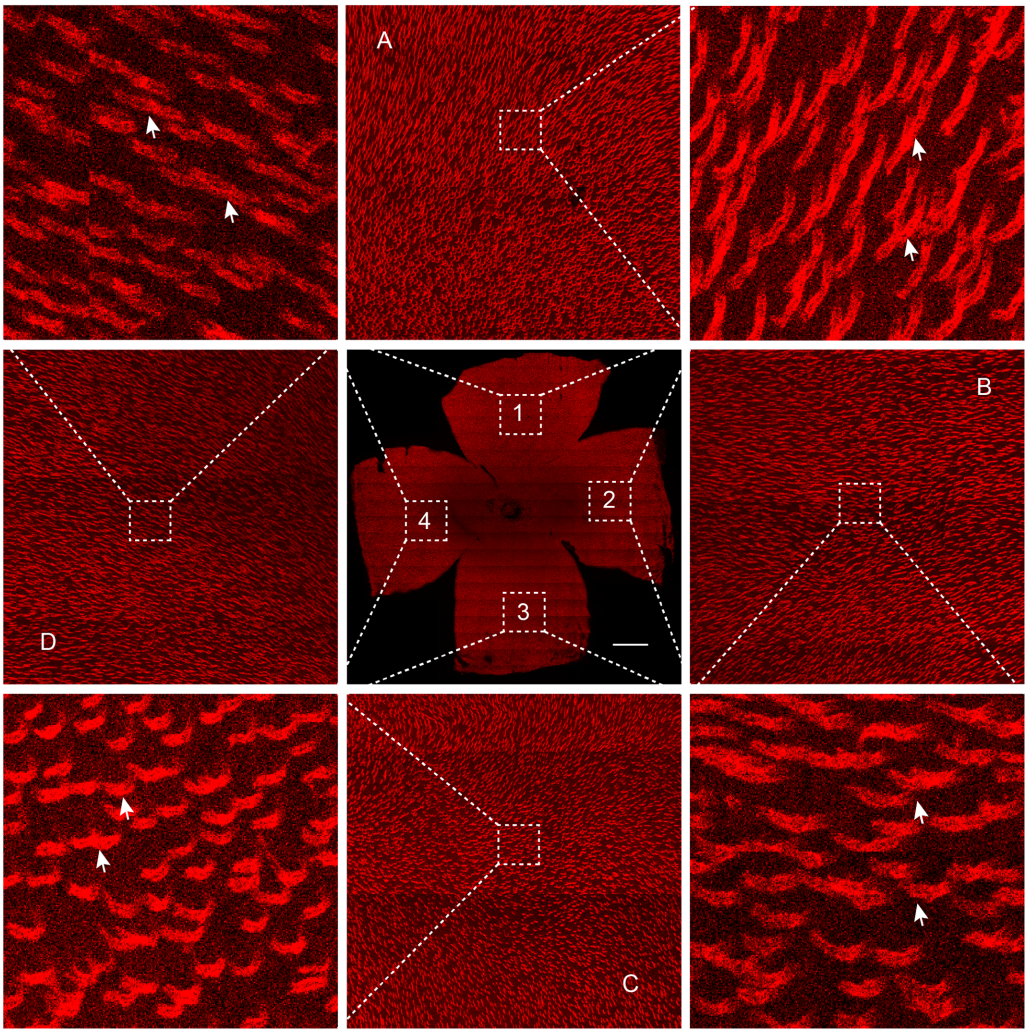

Figure 6. Six-month-old retina wholemount labeled with PNA. (**A**) Sequential magnification of the corresponding area 1 on the wholemount, highlighting the distribution of PNA in the retinal layers. (**B**) Sequential magnification of the corresponding area 2 on the wholemount, showing detailed PNA expression. (**C**) Sequential magnification of the corresponding area 3 on the wholemount, illustrating specific regions of PNA concentration. (**D**) Sequential magnification of the corresponding area 4 on the wholemount, indicating areas of interest with high PNA signal. *Scale bar* = 10 µm. *Arrowheads* indicate features associated with increased scores.

of 6-month-old and 12-month-old mice showed that the new method provided clear structure, clean background, and complete wholemounts, making it suitable for retinal studies in mice of different ages (Figs. 6, 7).

In summary, the newly developed method significantly reduced processing time and improved the quality of both retinal and RPE wholemounts. Compared with traditional methods, the new approach not only enhances whole mount integrity but also ensures the accuracy of staining and the preservation of cell morphology. These advantages make this method highly applicable in a wide range of research settings, especially in experiments that require detailed morphological analysis.

Discussion

This study introduces a simple, rapid, and effective method for simultaneously isolating mouse retina and RPE wholemounts. The method's simplicity, combined with its ability to preserve tissue integrity, makes it a valuable tool for ophthalmic research. Compared with traditional methods, this technique offers the following advantages: (1) simplicity: the process involves straightforward steps that do not require complex equipment or extensive training; (2) time efficiency: the entire procedure, from euthanasia to mounting, takes only 2 to 5 minutes per sample, allowing for high-throughput studies; and (3) high-quality whole-

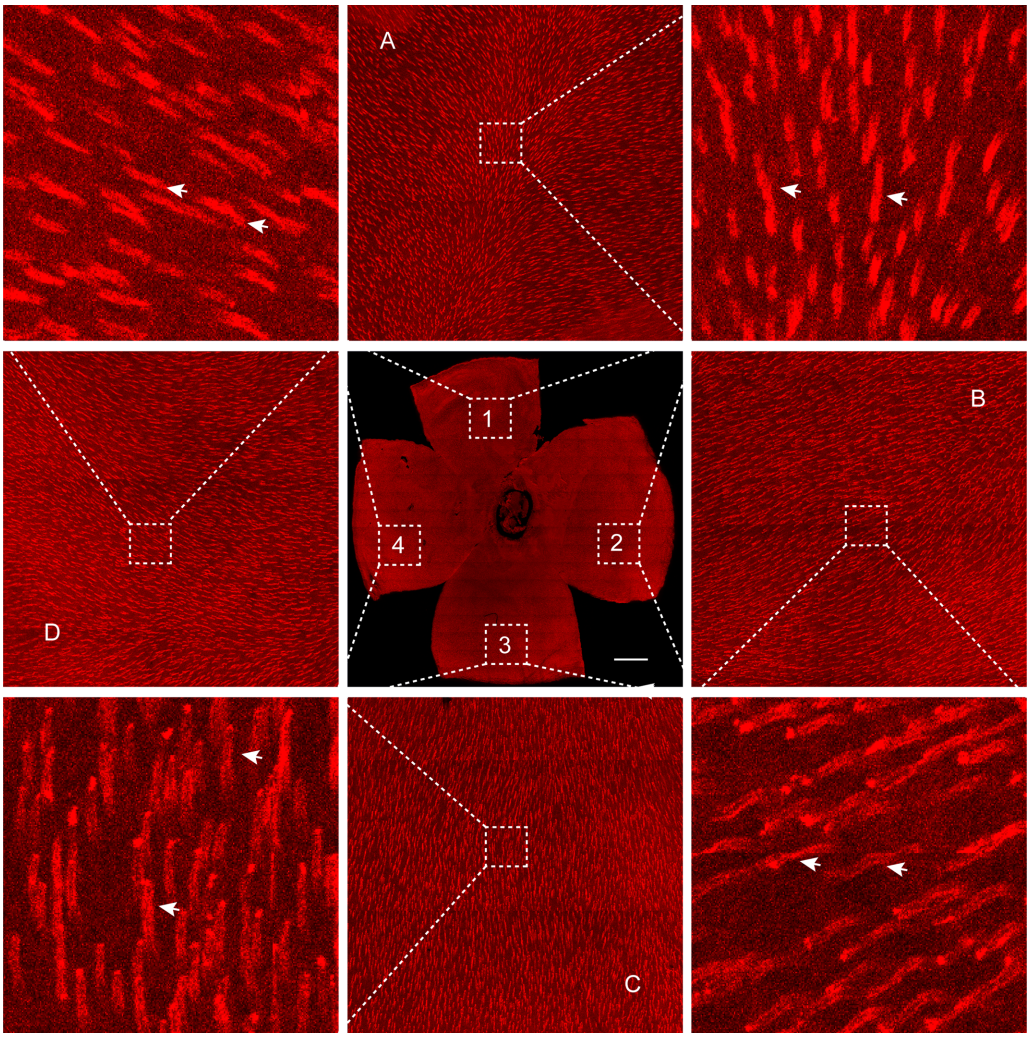

Figure 7. **Twelve-month-old retina wholemount labeled with PNA.** (**A**) Sequential magnification of the corresponding area 1 on the wholemount, depicting the spatial distribution of PNA in the retina. (**B**) Sequential magnification of the corresponding area 2 on the wholemount, highlighting areas of PNA expression. (**C**) Sequential magnification of the corresponding area 3 on the wholemount, focusing on PNA distribution patterns. (**D**) Sequential magnification of the corresponding area 4 on the wholemount, with arrows indicating regions of significant PNA presence. *Scale bar* = 10 µm. *Arrowheads* indicate features associated with increased scores.

mounts: the method consistently yields intact retina and RPE wholemounts, essential for high-resolution imaging and detailed analysis.

The method's robustness across different experimental setups underscores its potential for broader application. In practical applications, fixation time, tissue integrity, and morphology may be influenced by different disease models, particularly in preclinical models of diabetic retinopathy and AMD. In these disease states, the retina and RPE may exhibit distinct pathological features, such as cellular degeneration, tissue edema, and inflammatory responses.[14–19] These pathological changes can affect the tissue's structure and morphology, thereby posing new requirements for fixation time and processing methods. Future research could further optimize this technique for different species or experimental conditions, potentially enhancing its utility in diverse ophthalmic studies.

This study demonstrates a simple, rapid, and effective method for simultaneously isolating mouse retina and RPE wholemounts. The method's efficiency and ability to produce high-quality wholemounts offer a significant advancement in ophthalmic research, with implications for both basic and clinical applications.

Acknowledgments

Supported by the Sichuan Provincial People's Hospital (30320230095, J.Y.; 30420220062, J.Y.; and 2023BH12, H.W.). Additional support was provided

by the Natural Science Foundation of Sichuan Province (2024NSFC1719, J.Y.; 30420230353, J.Y.; and 2024NSFSC1541, H.W.). The 2022 Doctoral Research Start-up Fund Program (2022-BS-252, J.Y.). Postdoctoral Talent Innovation Program (BX202320, J.Y.).

Author Contributions: J.Y., Y.P., and Q.L., designed and performed experiments and analyzed the data. J.G., J.Y., S.P., X.W., H.H., R.C., J.C., and Y.W. recruited the participants and performed the ophthalmic examination. J.H., F.W., and H.W. conceived the project, designed the experiments, and supervised the project. J.Y. wrote the first draft of the manuscript, and J.H. edited the manuscript.

Disclosure: **J. Yang**, None; **H. Wu**, None; **Q. Li**, None; **J. Guo**, None; **J. Yao**, None; **S. Pan**, None; **X. Wu**, None; **H. Huang**, None; **R. Chen**, None; **J. Chen**, None; **Y. Wang**, None; **Y. Peng**, None; **F. Wu**, None; **J. Hu**, None

[*] JY, HW, and QL contributed to this work equally.

References

1. Jayaram H, Kolko M, Friedman DS, Gazzard G. Glaucoma: now and beyond. *Lancet*. 2023;402(10414):1788–1801.
2. Datta S, Cano M, Ebrahimi K, Wang L, Handa JT. The impact of oxidative stress and inflammation on RPE degeneration in non-neovascular AMD. *Prog Retin Eye Res*. 2017;60:201–218.
3. Strauss O. The retinal pigment epithelium in visual function. *Physiol Rev*. 2005;85(3):845–881.
4. Jager RD, Mieler WF, Miller JW. Age-related macular degeneration. *N Engl J Med*. 2008;358(24):2606–2617.
5. Song P, Du Y, Chan KY, Theodoratou E, Rudan I. The national and subnational prevalence and burden of age-related macular degeneration in China. *J Glob Health*. 2017;7(2):020703.
6. Zhang J, Huo YB, Yang JL, et al. Automatic counting of retinal ganglion cells in the entire mouse retina based on improved YOLOv5. *Zool Res*. 2022;43(5):738–749.
7. Song P, Wang J, Bucan K, Theodoratou E, Rudan I. National and subnational prevalence and burden of glaucoma in China: a systematic analysis. *J Glob Health*. 2017;7(2):020705.
8. Meng M, Chaqour B, O'Neill N, Dine K, Sarabu N, Ying GS, et al. Comparison of Brn3a and RBPMS labeling to assess retinal ganglion cell loss during aging and in a model of optic neuropathy. *Invest Opthalmol Vis Sci*. 2024;65(4):19.
9. David EM, Pacharinsak C, Jampachaisri K, Hagan L, Marx JO. Use of ketamine or xylazine to provide balanced anesthesia with isoflurane in C57BL/6J mice. *J Am Assoc Lab Anim Sci*. 2022;61(5):457–467.
10. Nadal-Nicolas FM, Kunze VP, Ball JM, et al. True S-cones are concentrated in the ventral mouse retina and wired for color detection in the upper visual field. *Elife*. 2020;9:e56840.
11. Yue J, Khan RS, Duong TT, et al. Cell-specific expression of human SIRT1 by gene therapy reduces retinal ganglion cell loss induced by elevated intraocular pressure. *Neurotherapeutics*. 2023;20(3):896–907.
12. Khan RS, Baumann B, Dine K, et al. Dexras1 deletion and iron chelation promote neuroprotection in experimental optic neuritis. *Sci Rep*. 2019;9(1):11664.
13. Shindler RE, Yue J, Chaqour B, Shindler KS, Ross AG. Repeat Brn3a immunolabeling rescues faded staining and improves detection of retinal ganglion cells. *Exp Eye Res*. 2023;226:109310.
14. Fleckenstein M, Schmitz-Valckenberg S, Chakravarthy U. Age-related macular degeneration: a review. *JAMA*. 2024;331(2):147–157.
15. Chakravarthy U, Peto T. Current perspective on age-related macular degeneration. *JAMA*. 2020;324(8):794–795.
16. Forrester JV, Kuffova L, Delibegovic M. The role of inflammation in diabetic retinopathy. *Front Immunol*. 2020;11:583687.
17. Hu J, Dziumbla S, Lin J, et al. Inhibition of soluble epoxide hydrolase prevents diabetic retinopathy. *Nature*. 2017;552(7684):248–252.
18. Dorweiler TF, Singh A, Ganju A, et al. Diabetic retinopathy is a ceramidopathy reversible by anti-ceramide immunotherapy. *Cell Metab*. 2024;36(7):1521–1533.e5.
19. Wang X, Xu C, Bian C, et al. M2 microglia-derived exosomes promote vascular remodeling in diabetic retinopathy. *J Nanobiotechnology*. 2024;22(1):56.